

## Reaction $^{55}\text{Mn}(p, n)^{55}\text{Fe}$ from $E_p = 1.35$ to $5.42$ MeV

Y. P. Viyogi, P. Satyamurthy, and N. K. Ganguly

*VEC Project, Bhabha Atomic Research Centre, Bombay 400085, India*

S. Kailas, S. Saini, and M. K. Mehta

*Nuclear Physics Division, Bhabha Atomic Research Centre, Bombay 400085, India*

(Received 15 August 1977)

The total  $(p, n)$  reaction cross section for  $^{55}\text{Mn}$  has been measured as a function of proton energy in the energy range 1.35 to 5.42 MeV with fine resolution ( $\sim 5$  keV). Several strong isobaric analog resonances have been located in the excitation function. The excitation function, averaged over a 200 keV energy interval has been compared with the optical model, Hauser-Feshbach, and Hauser-Feshbach-Moldauer calculations. The strong isobaric analog resonance at  $E_p \sim 1.54$  MeV has been shape analyzed to extract the proton width  $\Gamma_p$ , the spreading width  $W$ , the spectroscopic factor, and the reduced normalization.

[NUCLEAR REACTIONS  $^{55}\text{Mn}(p, n)$ ,  $E_p = 1.35$ – $5.42$  MeV; measured  $\sigma(E)$ ; optical model and Hauser-Feshbach analysis, isobaric analog resonance analysis.]

### I. INTRODUCTION

In continuation of our program of studies of  $(p, n)$  reactions below the Coulomb barrier on medium weight nuclides<sup>1,2</sup> through measurement of excitation functions, the total  $(p, n)$  cross section for the reaction  $^{55}\text{Mn}(p, n)^{55}\text{Fe}$  has been measured in the bombarding energy range from 1.35 to 5.42 MeV with fine resolution ( $\sim 5$  keV). The major motivation as discussed in Ref. 1 was to determine the optical model parameters for the target plus proton system at sub-Coulomb energies and to study in detail the isobaric analog resonances (IAR) observed.<sup>2-4</sup> Johnson, Galonsky, and Inskeep<sup>5</sup> have measured the thick target ( $\sim 75$  keV) excitation function for this reaction up to  $\sim 5.5$  MeV. Other previous studies of this reaction at these energies have been mainly confined to neutron and  $\gamma$  ray yield measurements for IAR studies.<sup>6,6(a)</sup>

The experimental arrangement, procedure, and results are discussed in Sec. II, while the analysis of the measured data is discussed in Sec. III followed by the conclusions given in Sec. IV.

### II. EXPERIMENTAL PROCEDURE AND RESULTS

The experimental technique and procedure followed in this measurement were the same as those for the earlier measurements described in Ref. 1. The targets prepared by evaporating natural manganese (100%  $^{55}\text{Mn}$ ; other metallic impurities  $\sim 20$  ppm) on tantalum backings were placed at the center of a  $4\pi$  geometry flat response neutron counter.<sup>7</sup> Proton beams of energy ranging from 1.35 to 5.42 MeV, available from the 5.5 MeV Van de Graaff accelerator at our laboratory, were used to bombard the targets. The beam current was in-

tegrated by a current integrator<sup>8</sup> and the total neutron yield was measured by the  $4\pi$  counter. The absolute cross section for the  $(p, n)$  reaction on  $^{55}\text{Mn}$  was measured over the bombarding energy range in steps of 5 keV with a target about 5 keV thick for 4 MeV protons. The resulting excitation function is shown in Fig. 1. In order to determine the shape of the strong IAR observed around 1.54 MeV with fine resolution, the excitation function was remeasured in that energy region with 1 keV steps and a thinner target ( $\sim 1$  keV for  $E_p = 2$  MeV). Two independent passes were made over the resonance to reduce the uncertainties arising due to target nonuniformities and beam energy fluctuations. The results are shown in Fig. 2. The target thickness was determined with an error of  $\pm 15\%$ , utilizing the back scattering technique described in Ref. 1. The maximum error in the absolute cross section is estimated to be  $\pm 20\%$ , comprising errors in target thickness determination: 15%; target nonuniformity: 5%; the efficiency<sup>9</sup> of the  $4\pi$  counter: 7%; current integration: 1%; and counting statistics: 2%.

It can be seen from Fig. 1, that the excitation function exhibits strong resonances as well as weaker fine structures having widths around 10 keV. The arrows indicate the expected positions of IARs assuming the Coulomb displacement energy  $\Delta E_c(^{56}\text{Fe}-^{56}\text{Mn}) = 8.590$  MeV. The IARs observed in the lower energy region by previous workers<sup>6</sup> are also seen in the present work, except for the analog of the ground state of  $^{56}\text{Mn}$  which is expected at about 1.34 MeV. Due to the difficulty in running the accelerator at energies below 1.5 MeV, the excitation function could not be extended to lower energies. At higher energies some of the stronger resonances can be correlated with the ex-

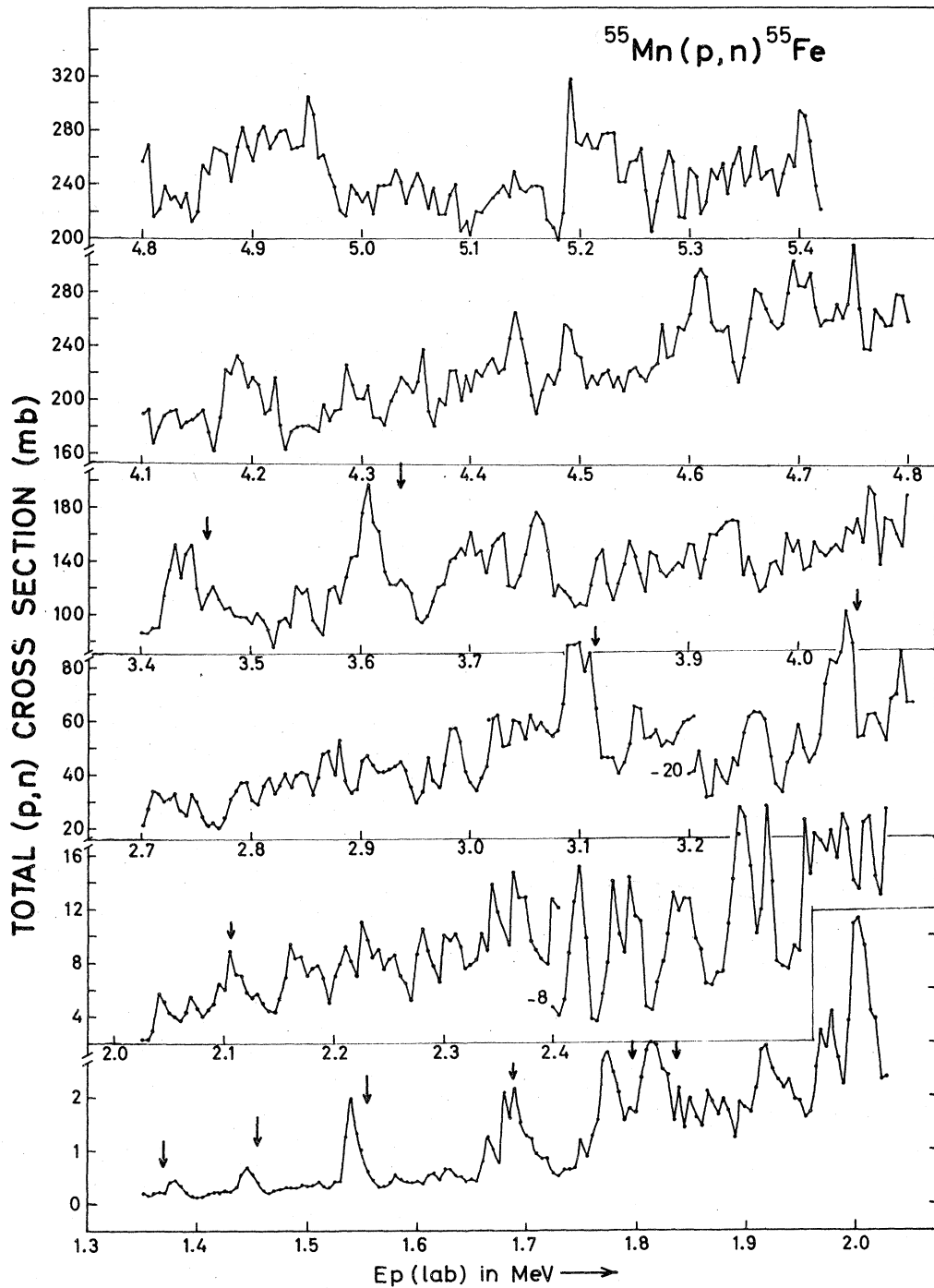


FIG. 1. Fine structure excitation function for the reaction  $^{55}\text{Mn}(p,n)^{55}\text{Fe}$  measured in 5 keV steps from  $E_p = 1.35$  to 5.42 MeV. The arrows indicate the expected positions of IAR based on the Coulomb energy shift  $\Delta E_C = 8.590$  MeV. Note the change in cross section scale at 2.4 and 3.2 MeV.

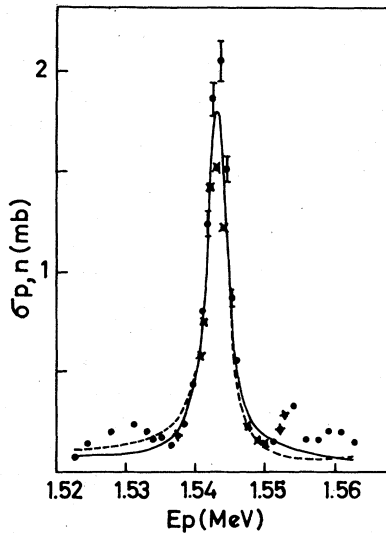


FIG. 2. Shape of the IAR at  $E_p \sim 1.54$  MeV measured with the  $\sim 1$  keV target. The dots and crosses represent two separate runs over the resonance. The continuous curve is the fit to data with the Breit-Wigner formula with  $\sigma_{\max} \sim 1.72$  mb,  $E_0 \approx 1.543$  MeV, and  $\Gamma_0 \approx 3.4$  keV. The dashed curve is the fit to data with the Robson-Johnson (RJ) formula (Ref. 3), with  $T_p^* = 0.000\,0525$ ,  $\Delta \approx -22$  keV,  $E_0 \approx 1.543$  MeV, and  $\Gamma_0 \approx 3.3$  keV.

pected positions of IARs; however, for many cases the structure observed around the arrow mark is weak. This indicates that the special significance of IAR is lost as the excitation energy increases.

No presence of any intermediate structure was noted when the excitation function was averaged over 100 and 200 keV energy intervals as can be seen from Figs. 3(a) and 3(b), respectively. The averaged  $\sigma_{p,n}$  values agree well with those of Johnson *et al.*<sup>5</sup>

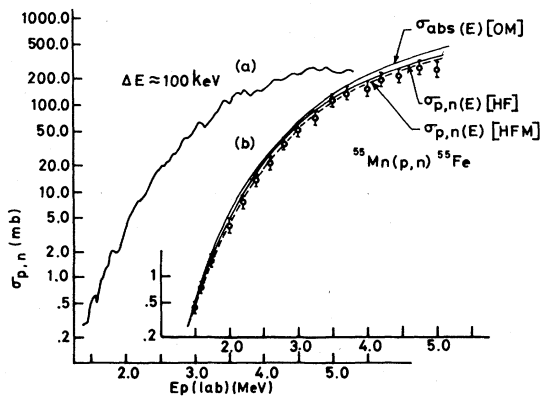


FIG. 3. (a) The fine structure excitation function averaged over 100 keV energy interval. (b) Optical model  $\sigma_{\text{abs}}(E)$  (OM), Hauser-Feshbach  $\sigma_{p,n}(E)$  (HF), and Hauser-Feshbach-Moldauer  $\sigma_{p,n}(E)$  (HFM) fits to the  $^{55}\text{Mn}(p,n)^{55}\text{Fe}$  reaction excitation function averaged over the  $\sim 200$  keV energy interval.

### III. ANALYSIS

#### A. Optical model and Hauser-Feshbach analysis

The fine structure excitation function of Fig. 1 was averaged over a 200 keV energy interval and compared with the optical model (OM) predictions following the procedure described in Ref. 1, assuming  $\sigma_{\text{abs}} \approx \sigma_{p,n}$ . Preliminary results of this analysis have been reported earlier.<sup>10</sup> The computer codes OMGLOB<sup>11</sup> and HAUFES<sup>12</sup> were used to calculate the total reaction cross section predicted by optical model and  $\sigma_{p,n}$  predicted by Hauser-Feshbach (HF) theory, respectively. The proton parameters of Becchetti and Greenlees<sup>13</sup> were used as the initial set. No spin orbit potential was used because the total reaction cross section is insensitive to such potentials. The imaginary potential depth  $V_I$  was decreased to 5 MeV in accordance with our previous experience with  $^{54}\text{Cr}$  and  $^{59}\text{Co}$  (Ref. 1). The data were then fitted with the optical model using least squares search technique varying  $V_I$ . The search on the radius and diffuseness parameter of the imaginary potential did not improve the fits appreciably. The fits to the data are shown in Fig. 3(b). It is seen that at lower energies the total cross section predicted by the optical model and  $\sigma_{p,n}$  (experimental) are very similar, thus verifying the assumption that at these energies the relation  $\sigma_{\text{abs}} \approx \sigma_{p,n}$  is valid. At higher energies however,  $\sigma_{\text{abs}}$  is higher than experimental values, and the more accurate HF calculation, with the same proton optical model potential and Wilmore and Hodgson's local equivalent neutron potential,<sup>14</sup> fitted the data very well. The inclusion of Moldauer's level width fluctuation correction<sup>15</sup> (HFM) in the HF calculation, however, did not improve the fit appreciably. The optical model parameters determined through this procedure and used for calculating the fits in Fig. 3(b) are listed in Table I.

TABLE I. Optical model parameters used for calculating the fits shown in Fig. 3(b). The proton parameters are determined in this work, as described in the text, starting with those given in Ref. 13. The neutron parameters are taken from Ref. 14.

	$^{55}\text{Mn} + p$	$^{55}\text{Fe} + n$
$V_R$	$58.8 - 0.32E_p$	47
$R_R$	1.175	1.3
$a_R$	0.75	0.62
$V_I$	$6 - 0.25E_p$ <sup>a</sup>	5 <sup>b</sup>
$R_I$	1.32	0.71
$a_I$	0.574	0.62

<sup>a</sup> Woods-Saxon derivative form for  $V_I$ .

<sup>b</sup> Gaussian form for  $V_I$ .

As in the previous work<sup>1</sup> the only significant departure of the present results from the optical model parameters determined at higher energies<sup>13</sup> has been the much lower value of  $V_I$ , the depth of imaginary potential. The energy dependence of  $V_I$  given in Ref. 13 would yield a value of  $V_I \approx 12$  MeV for a 4 MeV bombarding energy while the best fit value from our analysis yields a value of  $\sim 5$  MeV for  $V_I$  at that bombarding energy. It is understandable that  $V_I$  should be smaller at lower energies as the level density is very much reduced at the corresponding low excitation energies.

#### B. Shape analysis and extraction of spectroscopic factor for the IAR at 1.54 MeV

The strong resonance measured at 1.54 MeV and shown in Fig. 2 can be identified as the IAR formed by an  $l=1$  proton leading to a  $2^+$  level in the compound nucleus  $^{56}\text{Fe}$  which is the analog of the 0.213 MeV level in the parent nucleus  $^{56}\text{Mn}$ , studied through  $^{55}\text{Mn}(d, p)^{56}\text{Mn}$  reaction.<sup>16</sup> However, the subsequent  $(n, \gamma)$  measurement<sup>17</sup> on  $^{55}\text{Mn}$  has revealed that the parent state in question is a doublet with energies 212 and 215 keV with spins  $4^+$  and  $1^+$  or  $2^+$ , respectively. Similarly, the  $^{55}\text{Mn}(p, \gamma)^{56}\text{Fe}$  work<sup>6(a)</sup> has shown that there are two levels in  $^{56}\text{Fe}$  at  $E_x = 11699$  and  $11705$  keV with spins  $4^+$  and  $2^+$ , respectively, which could be the isobaric analogs of 212 and 215 keV levels of  $^{56}\text{Mn}$ . In the present  $(p, n)$  work, as our energy resolution is better than 2 keV, two levels separated by 6 keV as measured in  $(p, \gamma)$  work should be seen distinctly. However, there is no evidence for a second resonance in the neighborhood of the peak at 1.543 MeV as seen in Fig. 2 where the width of the resonance is only 3 keV. Considering the spins of the levels concerned, it can be seen that the  $4^+$  levels (the lower of the doublet) would be only weakly excited as a resonance in the  $(p, n)$  excitation function because of the extremely reduced penetrability of the partial wave for the outgoing neutron channel. Assuming that only the ground state of the residual nucleus  $^{55}\text{Fe}$  [with  $J^\pi = (\frac{3}{2}^-)$ ] would be energetically open for  $E_p = 1.54$  MeV, the outgoing neutron from the  $4^+$  IAR would have an energy of about 400 keV and would have to carry away an angular momentum of three units. The penetrability for this partial wave would be negligible compared with that for the neutron coming out due to the decay of the  $2^+$  IAR which would have similar energy but would have to carry away an angular momentum of one unit only. Thus the observed single strong resonance could be interpreted as the analog of the 215 keV  $2^+$  state of the parent nucleus  $^{56}\text{Mn}$ . This is in fact supported by the  $(p, n)$  and  $(p, \gamma)$  measurement of Otto *et al.*<sup>6</sup>

where one finds only one structure at this proton energy in the  $(p, n)$  reaction but more than one structure in the case of the  $(p, \gamma)$  reaction.

After having established the fact that only one of the two IARs in this energy region is observed in the  $(p, n)$  reaction, a detailed shape analysis of this IAR has been performed following (a) Robson-Johnson (RJ)<sup>3</sup> and (b) Breit-Wigner (BW) methods to extract the proton partial width  $\Gamma_p$ , spreading width  $W$ , and neutron spectroscopic factor  $S_n$ . The extraction of the IAR parameters and  $W$  was performed in the manner as described in Ref. 2. In Fig. 2 the theoretical fits to the data based on RJ and BW methods are shown, and as expected both approaches yield nearly equivalent fits to the data (as discussed by Jones,<sup>18</sup> at sub-Coulomb energies the Robson-Johnson expression reduces to the conventional Breit-Wigner formula). The  $\Gamma_p$  and  $W$  values are calculated as a function of channel radius and are shown in Fig. 4. As expected these values depend significantly on the channel radius. It is seen that  $\Gamma_p$  passes through a minimum at  $R \sim 4.25$  fm. Corresponding to this radius the optimum  $\Gamma_p$  and  $W$  values are  $0.0078 \pm 0.0001$  and  $2.50 \pm 0.03$  keV, respectively. The partial width extracted from BW analysis are as follows:

$$\Gamma_1 = 0.0075 \pm 0.0002 \text{ keV,}$$

$$\Gamma_2 = 3.39 \pm 0.06 \text{ keV.}$$

The  $\Gamma_p$  extracted from the RJ formula is very nearly equal to the value of  $\Gamma_1$  extracted from the BW analysis. The larger of the partial widths  $\Gamma_2$  in the BW analysis is of the order of the spreading width  $W$  extracted from the RJ procedure. We thus find that combining these two methods of analyses,

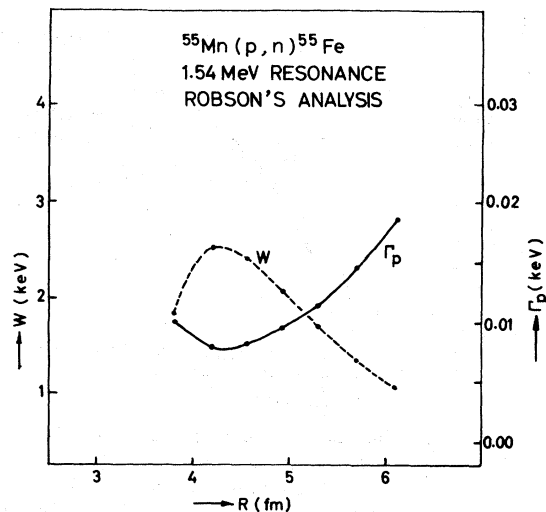


FIG. 4. Variation of  $\Gamma_p$  and  $W$  as a function of the channel radius  $R$ .

an unambiguous value of  $\Gamma_p$  can be obtained. The present results are similar to those obtained by Mehta *et al.*<sup>2</sup> in their analysis of the IAR in the  $^{51}\text{V}(p,n)^{51}\text{Cr}$  reaction. The mean value of  $\Gamma_p$  determined in the present analysis is  $0.0076 \pm 0.0002$  keV. The errors quoted on the values of  $\Gamma_p$  and  $W$  are those determined from the fitting procedure and reflect the scatter of points (i.e., statistical and uncertainties due to nonuniformity of the target). The absolute errors on these quantities, however, would have a maximum value of  $\pm 15\%$  reflecting the absolute error in the cross section measurement. The absolute error quoted here is smaller (thick target excitation function has an error of  $\pm 20\%$ ) as the thinner target thickness has been measured with an error of  $\pm 10\%$  as compared with the thick target measurement which has an error of  $\pm 15\%$  (Sec. II).

Thompson, Adams, and Robson<sup>19</sup> have discussed the relationship between  $\Gamma_p$  for an IAR and the corresponding spectroscopic factor  $S_n$  for the parent state, which can be utilized to determine  $S_n$  in the present case. In addition to  $\Gamma_p$ , this calculation involves the proton plus target (analog nucleus) and neutron plus target (parent nucleus) optical parameters and the proton channel radius  $a_c$ . It can be seen that  $S_n$  determined this way will be dependent on all these quantities. In order to study the sensitivity of the value of  $S_n$  to change in the neutron plus target optical parameters, especially the radius parameter ( $r_{n0}$ ) and the diffuseness parameter ( $a_n$ ),  $S_n$  values were calculated for a set of  $r_{n0}$  and  $a_n$  values in the following manner. For each value of  $r_{n0}$  and  $a_n$ , the  $S_n$  was calculated as a function of  $a_c$  utilizing the computer code SSEARCH<sup>20</sup> based on the expressions given in Ref. 19. In general  $S_n$  is expected to go through a minimum<sup>19</sup> as a function of  $a_c$ . It was found that this was not true in case of some  $r_{n0}$  values. However, in all cases the  $S_n$  versus  $a_c$  curves exhibited a plateau, where the values of  $S_n$  became insensitive to variation in  $a_c$ . This value of  $S_n$  (corresponding to  $a_c \sim 6.4$  fm in the present case) was chosen as an indicative value to study its variation with  $r_{n0}$  and  $a_n$ . Results of these calculations are shown as curves numbered (3) and (4) in Fig. 5 which indicate the strong dependence of  $S_n$  on  $r_{n0}$  and  $a_n$ . The  $S_n$  value was not very sensitive to the proton optical model parameters. The parameter set used in this calculation is given below:

$$V_R = 58.0, \quad R_R = 1.175, \quad a_R = 0.65 = a_{s0}$$

$$V_{s0} = 6.0, \quad R_{s0} = 1.2.$$

The spectroscopic factor obtained from the  $(d,p)$  reaction is also similarly dependent upon neutron potential parameters.<sup>21</sup> We have reanalyzed the

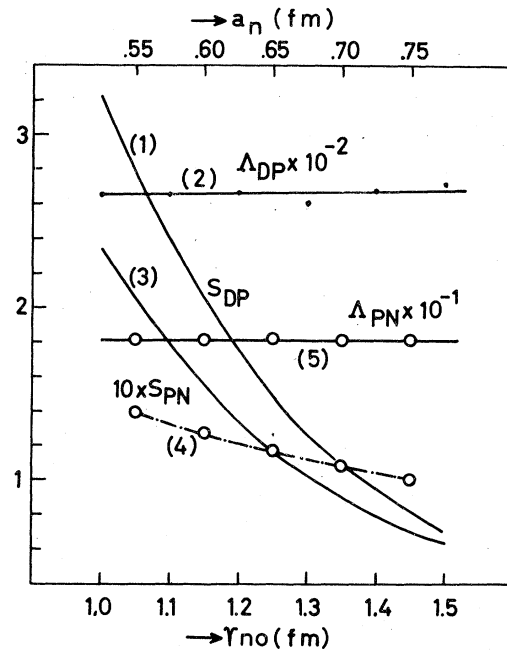


FIG. 5. Variation of spectroscopic factor  $S$  and reduced normalization  $\Lambda$  with  $r_{n0}$  and  $a_n$ . Curves numbered (1) and (2), respectively, show the variation of  $S_{DP}$  and  $\Lambda_{DP}$  as a function of the neutron radius parameter  $r_{n0}$  ( $a_n$  fixed at 0.65 fm). Curves numbered (3) and (4), respectively, show the variation of  $S_{PN}$  with  $r_{n0}$  ( $a_n = 0.65$  fm) and with  $a_n$  ( $r_{n0}$  fixed at 1.25 fm). Curve numbered (5) gives the variation of  $\Lambda_{PN}$  with  $r_{n0}$  ( $a_n$  fixed at 0.65 fm). The subscripts  $DP$  and  $PN$  refer to the spectroscopic factor extracted from  $(d,p)$  and  $(p,n)$  data, respectively.

$^{55}\text{Mn}(d,p)^{56}\text{Mn}$  reaction data of Comfort<sup>16</sup> (pertaining to the state at 0.213 MeV which is the parent of the present IAR) using his potential parameters and the code DWUCK<sup>22</sup> to obtain neutron spectroscopic factors for the parent state for various values of  $r_{n0}$ . The variation of this  $S_n$  (called  $S_{DP}$  in Fig. 5) with  $r_{n0}$  is also shown as curve numbered (1) in Fig. 5 for comparison with  $S_n$  (called  $S_{PN}$  in Fig. 5) obtained from the present IAR study.

Comparison between the spectroscopic factors extracted from  $(d,p)$  and IAR data is done better using the reduced normalization  $\Lambda$ <sup>21,23</sup> which is less sensitive to parameter variations. The quantity  $\Lambda$  has been obtained in the present work following the method of Clarkson, Von Brentano, and Harney,<sup>23</sup> where  $\Lambda \propto S_n |U_n|^2$ . Harney and Weidenmüller<sup>24</sup> have shown that  $S_n |U_n|^2$  ( $U_n$  being the normalized bound state neutron wave function) is independent of neutron potential parameters at a radius  $a_c$  where the proton wave function is zero. In the present investigation this value of  $a_c$  is again chosen at 6.4 fm, where  $S_n$  as a function of  $a_c$  shows a plateau as discussed earlier. The  $\Lambda$  val-

ues (called  $\Lambda_{PN}$ ) calculated by the above procedure<sup>23</sup> (utilizing the  $S_n$  values at  $a_c = 6.4$  fm) are also shown in Fig. 5 as a function of  $r_{n0}$ . It is found that the  $\Lambda_{PN}$  value is constant to within 1%. Similar calculations have been done for  $(d, p)$  data as well and in this case the value (called  $\Lambda_{DP}$ ) is found to be constant to within 4% as indicated in Fig. 5.

The above detailed discussion would indicate the difficulties in comparing the results of  $(d, p)$  and  $(p, n)$  analysis of the IARs due to the parameter dependence of  $S_n$ . The usefulness of the reduced normalization  $\Lambda$  in this regard is also demonstrated. However, the comparison between the corresponding numbers in the present case shows that the values of optimum  $S_n$  as well as  $\Lambda$  obtained in the present  $(p, n)$  analysis ( $S_{PN}$  and  $\Lambda_{PN}$ ) are lower by almost an order of magnitude compared with  $S_{DP}$  and  $\Lambda_{DP}$ . The disagreement up to a factor of 5 has been previously observed in such comparisons.<sup>25</sup> On the other hand, due to the fact that Comfort<sup>16</sup> in his  $(d, p)$  work has not resolved the doublet around 215 keV, the  $S_n$  obtained in this work would represent the combined strength of the two levels, while the present  $(p, n)$  work only measures the spectroscopic factor of the 215 keV  $2^+$  level. Van Assche *et al.*<sup>17</sup> in a study of the  $^{55}\text{Mn}(n, \gamma)^{56}\text{Mn}$  reaction have estimated the contribution from the two states and found only 40% being contributed by the  $2^+$  states. This would indicate a change in the values of  $S_n$  and  $\Lambda$  in the right direction to be consistent with the  $(p, n)$  results. The analysis technique described here has been subsequently used in a similar study of the  $^{80}\text{Se}(p, n)^{80}\text{Br}$  reaction<sup>26</sup> at our laboratory where the agreement between the  $S_{PN}$  and  $S_{DP}$  is very good. This work

also indicated that the analysis of IAR observed in the  $(p, n)$  reaction is likely to provide better spectroscopic factors than those obtained through  $(p, p)$  studies for resonances much below the Coulomb barrier.

#### IV. CONCLUSION

The present work has resulted in the determination of proton optical model parameters for  $^{55}\text{Mn}$  at sub-Coulomb energies through optical model and Hauser-Feshbach analysis of  $(p, n)$  excitation function. It is found that the value of the imaginary potential is smaller than that determined at higher energy. It should be mentioned again that this method of extraction of proton optical model parameters by fitting  $(p, n)$  data is most reliable at sub-Coulomb proton energies as the more conventional method of fitting the  $(p, p)$  angular distribution would not be suitable at these low energies due to large Coulomb effects. The  $S_n$  calculated from this work does not agree with that extracted from  $(d, p)$  work because of the fact that  $(d, p)$  deals with an unresolved doublet and the present work deals with only one of the two levels ( $2^+$  level) in the doublet.

#### ACKNOWLEDGMENTS

The help of Mr. C. V. Fernandes, Mr. V. V. Tambwekar, and Mr. A. Banerjee at various stages of the experiment is gratefully acknowledged. The authors also thank Mr. S. Pal for his help in running the DWUCK program. Thanks are also due to the Van de Graaff accelerator crew for their cooperation.

<sup>1</sup>S. Kailas, S. K. Gupta, M. K. Mehta, S. S. Kerekatte, L. V. Namjoshi, N. K. Ganguly, and S. Chintalapudi, *Phys. Rev. C* **12**, 1789 (1975).  
<sup>2</sup>M. K. Mehta, S. Kailas, and K. K. Sekharan, *Pramana* **9**, 419 (1977).  
<sup>3</sup>C. H. Johnson, R. L. Kernell, and S. Ramavataram, *Nucl. Phys.* **A107**, 21 (1968).  
<sup>4</sup>K. K. Sekharan and M. K. Mehta, *Phys. Rev. C* **6**, 2304 (1972).  
<sup>5</sup>C. H. Johnson, A. Galonsky, and C. N. Inskeep, ORNL Report No. ORNL-2910, 1960 (unpublished), pp. 25-28.  
<sup>6</sup>Bruce T. Murdoch, E. B. Paul, R. S. Blake, and B. E. Bonner, *Bull. Am. Phys. Soc.* **11**, 751 (1966); G. Otto, R. Mehnertard, and G. Tomaselli, *Nucl. Phys.* **A109**, 118 (1968); A. Ahmed, M. A. Rehman, M. A. Awal, M. Rehman, S. Khatum, and H. M. Sengupta, *Phys. Soc. Jpn.* **35**, 348 (1973).  
<sup>6(a)</sup>R. J. Peel, D. R. Dixon, M. W. Hill, G. L. Jensen, N. F. Mangelson, N. Nath, and V. C. Rogers, *Nucl.*

*Phys.* **A235**, 205 (1974).

<sup>7</sup>K. K. Sekharan, M.Sc. thesis, Bombay University, 1966 (unpublished).

<sup>8</sup>S. K. Gupta, *Nucl. Instrum. Methods* **60**, 323 (1968).

<sup>9</sup>S. K. Gupta and S. S. Kerekatte, Bhabha Atomic Research Center (BARC) Report No. 579, 1971 (unpublished).

<sup>10</sup>S. Kailas, Y. P. Viyogi, S. Saini, S. K. Gupta, N. K. Ganguly, M. K. Mehta, A. Banerjee, and S. S. Kerekatte, *Nucl. Phys. Solid State Phys. (India)* **17B**, 78 (1974); S. Kailas, Y. P. Viyogi, P. Satyamurthy, S. Saini, N. K. Ganguly, and M. K. Mehta, *ibid.* **18B**, 8 (1975).

<sup>11</sup>Y. P. Viyogi and N. K. Ganguly, BARC report (unpublished).

<sup>12</sup>Y. P. Viyogi and N. K. Ganguly, BARC Report No. I-361, 1976 (unpublished).

<sup>13</sup>F. D. Becchetti and G. W. Greenlees, *Phys. Rev.* **182**, 1190 (1969).

- <sup>14</sup>D. Wilmore and P. E. Hodgson, *Nucl. Phys.* 55, 673 (1964).
- <sup>15</sup>P. A. Moldauer, *Rev. Mod. Phys.* 36, 1079 (1964).
- <sup>16</sup>J. R. Comfort, *Phys. Rev.* 177, 1573 (1969).
- <sup>17</sup>P. H. M. Van Assche, H. A. Baader, H. R. Koch, B. P. K. Maier, U. Gruber, O. W. B. Schutt, J. B. McGrory, J. R. Comfort, R. Rimawi, R. E. Chrien, D. A. Wasson, and D. I. Garber, *Nucl. Phys.* A160, 367 (1971).
- <sup>18</sup>G. A. Jones, in *Isobaric Spin in Nuclear Physics*, edited by J. D. Fox and D. Robson (Academic, New York, 1966), p. 857.
- <sup>19</sup>W. J. Thompson, J. L. Adams, and D. Robson, *Phys. Rev.* 173, 975 (1968).
- <sup>20</sup>R. Van Bree (private communication).
- <sup>21</sup>J. Rapaport and A. K. Kerman, *Nucl. Phys.* A119, 641 (1968).
- <sup>22</sup>S. Pal (private communication).
- <sup>23</sup>R. G. Clarkson, P. von Brentano, and H. L. Harney, *Nucl. Phys.* A161, 49 (1971).
- <sup>24</sup>H. L. Harney and H. A. Weidenmuller, *Nucl. Phys.* A139, 241 (1969).
- <sup>25</sup>E. G. Bilpuch, A. M. Lane, G. E. Mitchell, and J. D. Moses, *Phys. Rep.* 28C, 145 (1976).
- <sup>26</sup>S. Kailas, N. K. Ganguly, M. K. Mehta, S. Saini, N. Veerabahu, and Y. P. Viyogi, Contributed paper, Proceedings of the International Conference on Nuclear Structure, Tokyo, 1977 (unpublished), p. 297.